

# Development of Low Emission Combustor for 110 MWe Gas Turbine

Lyudmila Bulysova, Vasily Vasiliev, Arkady Berne, Mikhail N. Gutnik\* and Mikhail M. Gutnik

All-Russia Thermal Engineering Institute, Moscow, Russia; bulysov@mail.ru, vdvasiliev@vti.ru, ariol.ltd@zmail.ru, mngutnik@vti.ru

## Abstract

**Background:** This is a review article. The stages of development and finishing of Low-Emission Combustor (LEC) for GTE-110 gas turbine with capacity of 110 MW are presented. The main problem referred to in the article is pressure pulsations arising in certain modes of LEC operation. **Methods:** A detailed account of numerical and experimental research is given for detection of contributing factors on arising of unstable combustion, leading to pressure pulsations with high magnitudes (more than 2% of air pressure at the inlet of LEC). A computational and experimental approach to research of processes in LEC is described. Method of influence upon the border of steady combustion area is shown. **Findings:** Relationship between position and shape of flame in the volume of flame tube and stability of combustion process is described. Design criterion of stable combustion, allowing comparison of modifications of LEC structures and operation modes is presented. Technical solution developed on the basis of calculation and experimental studies, allowing implementation of stable and low-emission operation of LEC in all design operation modes of Gas Turbine (GT), is presented. The results of tests at pressures up to 450 kPa in the form of diagrams of combustion efficiency and  $\text{NO}_x$  emissions over the entire load range of GT are presented. **Improvements:** Control method of combustor to achieve these characteristics was developed.

**Keywords:** 3D Simulation, Calculation Studies, Combustor, Experimental study, Flame Front, Fuel-Air Mixture, Gas Turbines, Low Emission Combustion, Pressure Pulsations, Transient Processes

## 1. Introduction

GTE-110 gas turbine power unit manufactured by NPO Saturn having unit capacity 110W is on par with the best world standards in terms of design. It is intended for use at electric power stations as part of combined cycle gas turbine units or for individual operation in a simple and cogeneration cycles with the generation of electric and thermal energy in the base, semi-peak and peak usage classes. However, increased pollutant emissions ( $\text{NO}_x$ ) currently hinder the rapid introduction of these gas turbines in the energy sector and industry.

It is found that operational conditions of gas turbine units influence exhaust gas emissions<sup>1</sup>. Intense studies are carried out to eliminate this drawback using lean fuel/air ratio<sup>2-5</sup>. Moreover, thermo-acoustic instabilities in GT combustor operation resulting in large pressure pulsations, poor combustion and combustor damage.

Numerous methods are offered to mitigate combustion driven instabilities<sup>6-9</sup>, but the problem remains relevant.

At the first stage of the LEC development for GTE-110M the concept of LEC creation was designed which implemented the decision to provide low emissions of nitrogen oxides by arranging effective combustion of 'lean' premixed fuel-air mixture. A number of computational studies were carried out with the use of software systems concerning the impact of aerodynamic and design parameters of the burner on the fuel-air mixture formation and burning in the low-  $\text{NO}_x$  combustion chambers of gas turbines. Evaluative calculations were conducted with regard to the intensification of convective cooling of Flame Tube (FT) walls in different ways.

During the first test series (iteration) works were carried out to determine start-up modes, the pressure losses in the combustion chamber and air distribution over the LEC path and non-uniformity of the temperature field

\*Author for correspondence

at the LEC output, to adjust the transition from the pilot burner to the main one, to study combined action modes of the pilot and main burners during fuel redistribution between them at 45-100 % load, to establish lean blowout of the pilot and main burners, the temperature state of the FT wall metal and to investigate backfire into the main burner of the LEC.

LEC test results showed that the main parameters are close to the designed characteristics, however, at a load of ~ 40% with fuel flow rate to the pilot burner making at least 20% of the total, pressure pulsations occurred with emergency amplitudes at 3400-3600 Hz and 2400-2600 Hz.

To overcome this problem, the research program was developed in the course of which the impact of the FAM concentration profile on NO<sub>x</sub> emission was determined, as well as the flame shape impact on the stability of the combustion process and transient processes. A criterion for vibrating combustion excitation was developed. In the option with FAM concentration enrichment toward the FT walls during experimental studies, CC pulsation-free operation was achieved during PB and MB combined action with any PFR.

Conducted computational studies and tests made it possible to find a technical solution which combined an option with the uniform FAM arrangement and an option with a distorted distribution diagram of FAM concentration, simultaneously met emission and stability requirements and did not require significant rework of the material. Based on these findings an algorithm for controlling LEC of GTE-110M was designed.

## 2. Concept Headings

Development of low emission combustors is one of the most topical and costly problems of modern gas-turbine development, especially for high power GT. Development of LEC is always a compromise between requirements on emissions of CO and NO<sub>x</sub>, aiming for simple producible structures, life extension, etc. High development costs of LEC are due to the lack of reliable methods of calculation of transient processes of flow and combustion even using modern computational tools. Therefore, experiments in LEC development are conducted on full-scale facilities at elevated air pressures, which require considerable expenses and time.

To test the LEC an experimental setup was designed and manufactured. The scheme of the experimental setup

is shown in Figure 1. The experimental setup consists of an inlet section (air inlet) (1), a test compartment (2) and a water-cooled measuring section (MS). Power compartment body is designed as a sector of the 1/20 part of GTE-110M combustion chamber housing and imitates its internal contours. The air is fed into the main volume of the test compartment through a rectangular duct at the bottom of the housing. Internal screens provide simulation of velocity distributions at the top and bottom of the compartment. The measuring section is directly connected to the compartment at the LEC transition liner outlet. A water-cooled nozzle (6) is installed at the MS outlet.

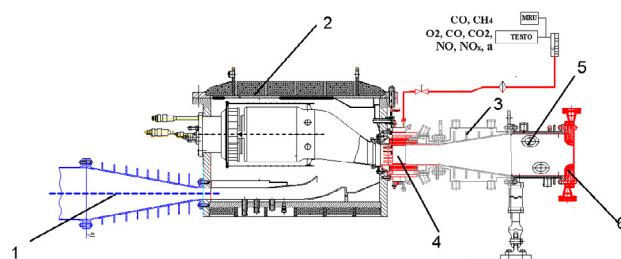


**Figure 1.** Scheme of the experimental setup.

1- Inlet section; 2- Test compartment; 3 – Measurement section; 4 – 1<sup>st</sup> cross-section; 5 – 2<sup>nd</sup> cross-section; 6 – water-cooled nozzle.

**Table 1.** LEC main parameters

Parameter	Dimension	Value
Air flow rate	kg/s	15.27
Input air pressure	kPa	1518.4
Input air temperature	K	675.8
Natural gas flow rate	kg/h	1149.45
Temperature of combustor discharge	K	1483.4

The composition and temperature of the exhaust gases are measured in the measuring section inlet (1<sup>st</sup> cross-section) (4). At this point, 5 water cooled probes are mounted on the bottom wall of the measuring section to measure flow temperature, and 6 probes are mounted on the top wall to take gas samples. There are 4 gas sampling probes arranged crosswise (2<sup>nd</sup> cross-section) (5) downstream.

Inlet air temperature is measured at three points along the length of the rectangular inlet duct; static pressure is measured in the test compartment cavity at two combined points. The walls of the flame tube are equipped with K type thermocouples.

Figure 2 schematically shows a longitudinal sectional view of designed LEC mounted in a test rig box. Its main parameters are summarized in Table 1. A widespread scheme of lean C with premixing and flame stabilization in swirl was chosen to ensure these parameters. The combustor has two co-axial burners – MB with radial swirler and PB with axial swirler (Figure 1). MB fuel is supplied through the holes in vanes of the swirler and is mixed with air in PZ, so that FT is supplied by well-mixed FAM. PB fuel enters directly into FT through the holes near the exit of axial swirler.

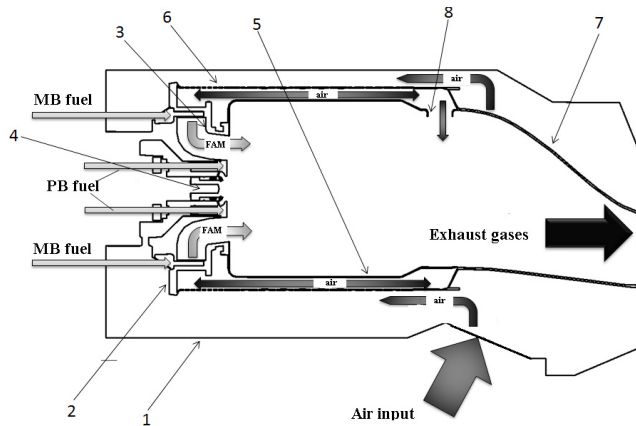


**Figure 2.** Sectional view of LEC, disposed in test compartment.

1 - Compartment; 2 - Burner arrangement (BA); 3 - Main burner (MB); 4 - Pilot burner (PB); 5 - Flame tube (FT); 6 - Cooling jacket; 7 - Gas collector; 8 - Mixer bushings.

**Table 2.** Air flow rate in the combustor

Parameter	Dimension	Value
MB air flow rate	%	65
PB air flow rate	%	6
SAT air flow rate	%	25
Air flow rate for gas collector cooling	%	4

Selected C scheme has a number of features. For clarity the C can be divided into three parts: 1) BA with supplies of fuel to MB and PB, 2) FT at the output of which SAH are located and 3) exit duct. Cooling of FT walls is impact with air fed through the holes in the cooling cowling. All air used for cooling comes to burners and SAH. FT does not have internal (film) cooling and this promotes uniform temperature distribution in combustion zone. Exit

duct has film cooling with supply of air through the orifices of small diameter. The hot part of C – FT and exit duct have no movable couplings, which in combination with extensive cooling system helps to extend the C life. The main parameters that determine the flow in C are presented in Table 2.

Selected parameters ensured compliance with requirements on emissions, temperature of metal and C pressure drop. At the same time the exit temperature non-uniformity of 1.3 substantially exceeded specified in PB operating modes, however maximum local temperature exceeded 1350°C.

For implementation of requirements for the C exit temperature uniformity, studies on optimization of secondary air injection were performed. Calculation was performed in Flow Vision software by finite element analysis. It became clear from parametric studies that elevated temperature in flow core was caused by insufficient efficiency of secondary air jets incoming through 6 SAH.

According to results of calculation, 3 rimmed SAH were made with the same total flow path area instead of initial 6 SAH. Irregularity of PB operation has decreased significantly, at that maximum local temperature was reduced by 260°C.

The main C test problem, as in many other known cases, appeared during tests at elevated pressures. It was high frequency pressure pulsations caused by unstable combustion, or combustion noise. Pulsations appeared during changeover from PB to MB, i.e., during reduction of PFR. Figure 2 shows pressure pulsation at stable (Figure 3(a)) and unstable (Figure 3(b)) modes and their corresponding frequency spectra.

Pulsation magnitude in some cases exceeded 3% of pressure in CC, which is unacceptable for structural strength of elements. Pulsation frequency was 2200-2500 Hz and 3300-3600 Hz, which clearly points to thermo-acoustic nature of process. Mathematical simulation of such processes requires calculations in unsteady approach, which are verified according to experiment.

Technology of experimental development of such C is not described in the literature and there is also no such experience in VTI. Therefore, for elaboration of test technology and comparison of tests with simulation results, a scaled simulator combustor was designed, manufactured and tested (Figure 4).

The scaled combustor is a simplified aerodynamic model of full scale C. Flow distribution and ratio of PB

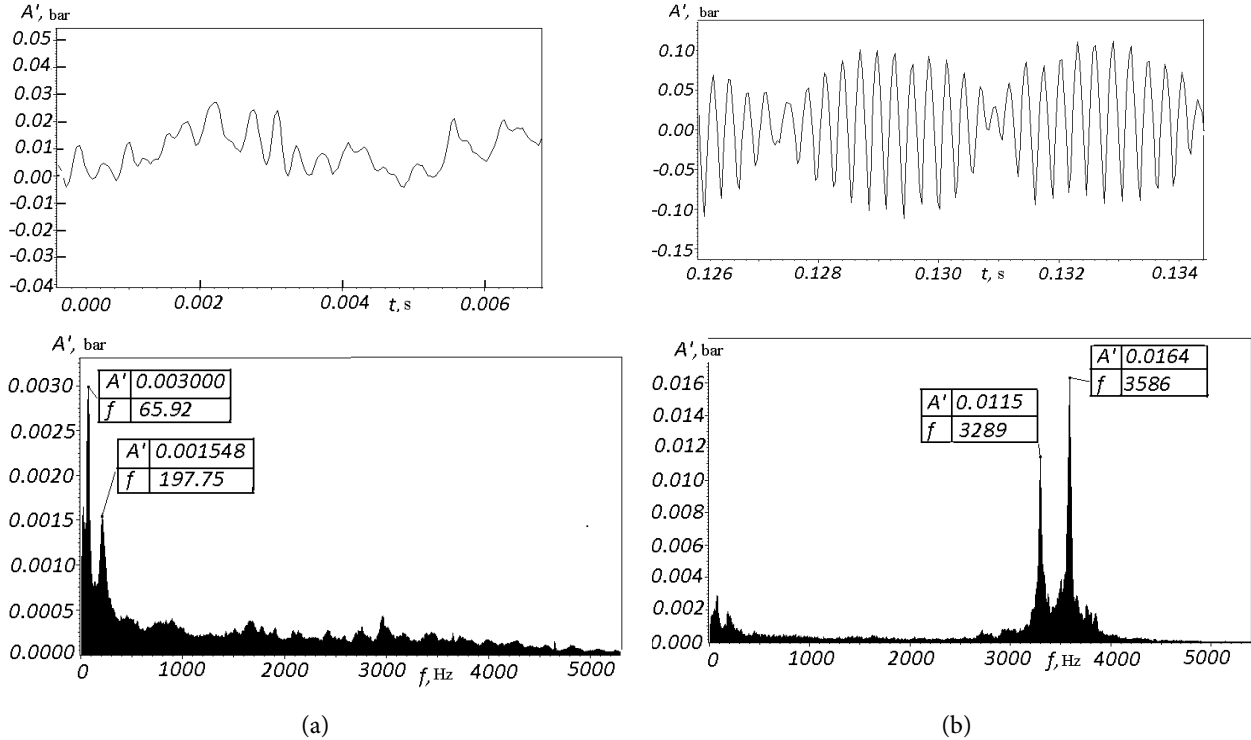


**Figure 3.** Signals of pressure pulsations and magnitude-frequency characteristic. (a) Mode of stable combustion N= 45%, PFR=30%. (b) Mode of combustion noise N= 45%, PFR=22%.

and MB flows, swirl characteristics, etc., are equal to parameters of full scale C, but mass flows of air and fuel are  $\sim 10$  times smaller. The simulator C is axially symmetrical, which allowed reducing substantially amount of calculations.

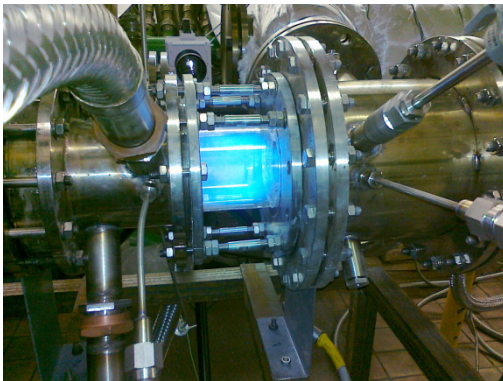


**Figure 4.** Test facility for the study of dynamic processes in low-emission combustors of stationary GT.

Technology of LEC testing was worked out on the simulator C, in particular technology of measurements and analysis of pressure pulsations; as well as quantitative criteria for reaching unstable combustion zone was formulated<sup>10</sup>.

Tests of the scaled C allowed obtaining a number of parametric relations also applicable to full scale LEC<sup>11,12</sup>. For example dependences, allowing estimating the heat release distribution along the C axis, i.e., the position of the flame, were obtained. Figure 5 shows the distribution of specific heat release ( $\bar{q}$ )<sup>13</sup> along the C axis ( $\bar{X} = \frac{x}{D}$ , where  $x$  is a current coordinate along C axis, measured from the end of PB,  $D$  – diameter of FT) depending on air excess factor ( $a$ ) during operation without support of pilot fuel (PFR=0).

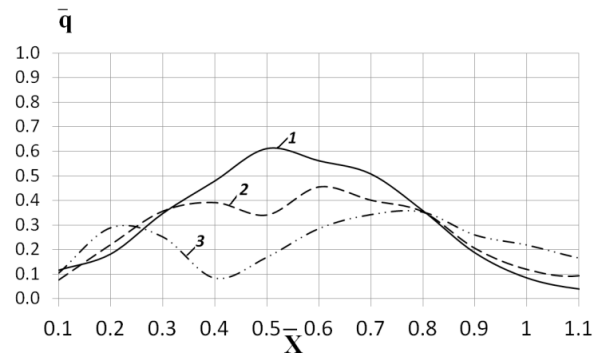


**Figure 5.** Distribution of specific heat release  $\bar{q}$  along the length of CC where PFR = 0: 1 –  $a = 1.93$ ; 2 –  $a = 2.0$ ; 3 –  $a = 2.2$ .

Calculations carried out by procedure, worked out on the pattern C, showed the presence of two zones of flame anchoring – central and corner (Figure 6).

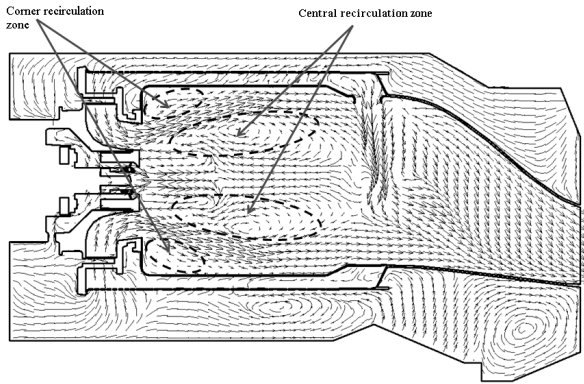


Figure 6. Velocity vectors in longitudinal section of LEC.

Central recirculation zone is produced by flow swirl in the swirler of MB and corner recirculation zone – by flow sudden expansion at the MB mixing channel exit.

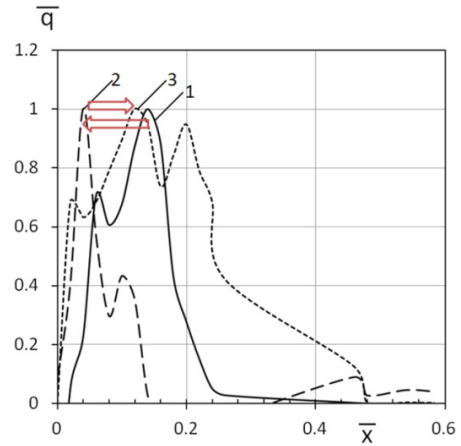


Figure 7. Specific heat release along the FT axis in case of: 1 – PFR=30%; 2 – PFR=24%; 3 – PFR=0%.

Analysis of flame movement, evaluated by position of specific heat release ( $\bar{q}$ ) peak along the axis of FT ( $\bar{X}$ ) in case of different values of PFR, showed that due to flame anchoring in either corner or central zones of reverse

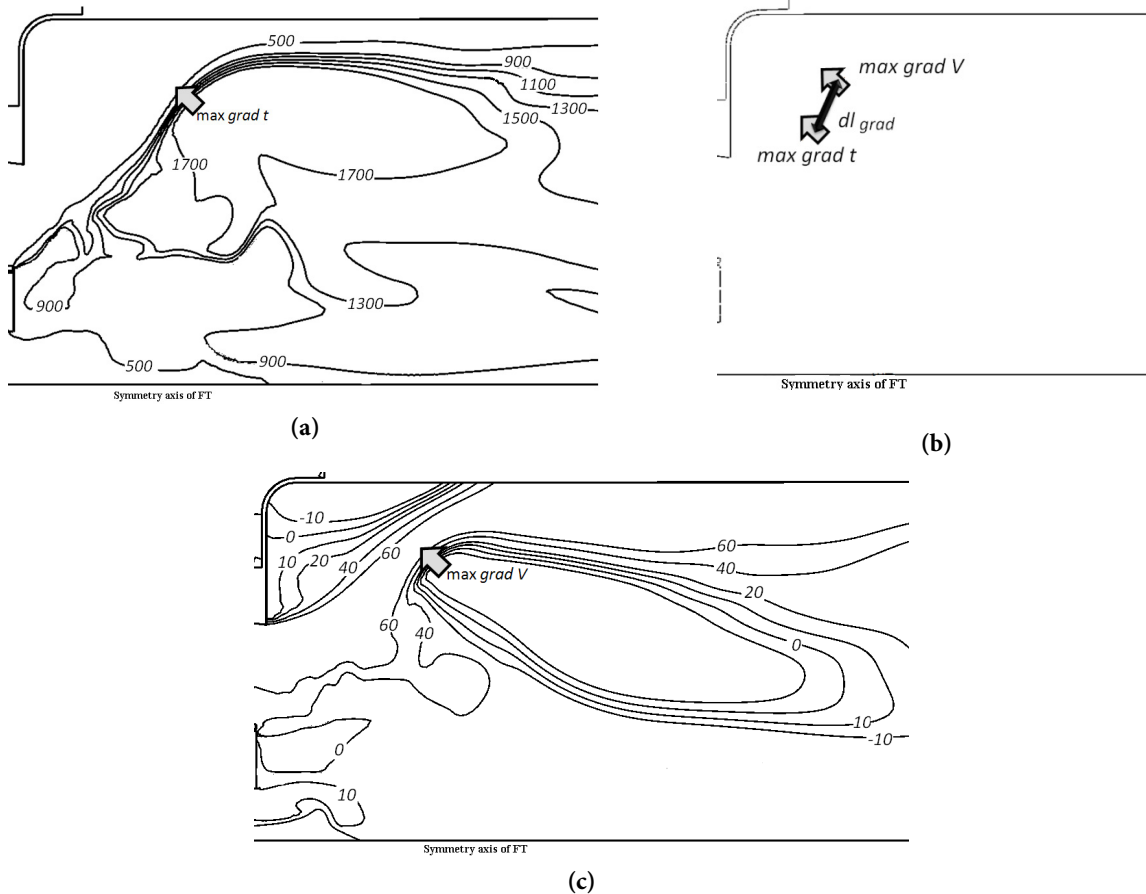


Figure 8. Isograms and location of gradient peaks of. (a) Temperature. (b) Axial velocity. (c) Relative position of maximum gradients of temperature and velocity and shortest distance between them.

flows, peak of specific heat release is farther from BA, and flame front surface is less developed than in simultaneous stabilization in two zones where fuel burns quickly in close proximity to BA (Figure 7).

High frequency combustion noise arises in case of simultaneous stabilization in two zones and/or unstable transition of anchoring from one zone to another. In turn, change of stabilization mode is accompanied by change of heat release along the C axis (Figure 7).

Calculations and experiments detected relation of combustion process stability with flow and heat release structures. Combustion instability is stimulated by zones of high turbulence or high velocity gradients, and by the flame front or zones of high temperature gradients.

Criterion of combustion noise stimulation was proposed in<sup>13</sup>. That work in<sup>13</sup> detected a relationship between the position and values of maximum velocity and temperature changes, evaluated by results of calculation studies and observed pressure pulsations in the combustor, measured experimentally. It is found that position and shape of flame front play a dominant role in the combustion stability. Near BA flow pattern is complex and there are areas with large local velocity changes  $\max grad(V)$  from -10 m/s to 130 m/s due to design of BA (swirling of flows in PB and MB, Figure 6). Approach of the flame front to these zones contributes to initiation of unstable combustion in LEC.

Analysis of LEC operation modes revealed that change of concentration distribution in the volume of FT by changing fuel split between PB and MB leads to a change in the position and shape of the flame front. At certain values of PFR (PFR = 24%, Figure 7) the flame front moves into the area of larger velocity gradients, which leads to combustion instability and arising of pressure pulsations.

Stimulation criterion of combustion noise is calculated as follows. Values and location of peaks of temperature and velocity gradients and distance between them are determined by steady state calculation of combustion process.

Relative position of peaks of temperature changes

$$\max grad(t) = \max \frac{dt}{dl} \text{ (Figure 8(a)) and changes in}$$

$$\text{axial velocity } \max grad(V) = \frac{dV}{dl} \text{ are taken into account}$$

in the proposed criterion of combustion stability (Figure 8(b)).

Stability criterion is stated as

$$\frac{\max grad(t) * \max grad(V)}{dl_{grad}},$$

Where  $dl_{grad}$  is a distance between peaks of gradients (Figure 8c).

$$\frac{\max grad(t) * \max grad(V)}{dl_{grad}},$$

Calculated value of stability is well-correlated with experimentally measured magnitudes of pressure pulsations. Results of experimental and calculation studies are shown in Table 3.

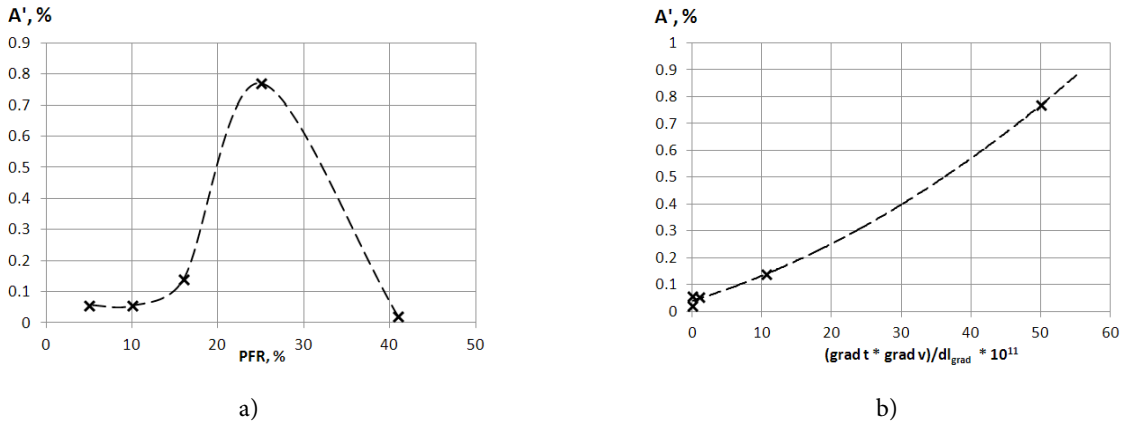
Figure 9(a) shows dependence of pressure pulsations magnitude upon PFR, obtained experimentally in mode with  $P_{inc} = 330 \text{ kPa}$ ,  $t_{inc} = 340^\circ\text{C}$ ,  $\alpha = 3.0$ . Peak of pressure pulsations is observed in case of PFR = 24%.

Figure 9(b) shows dependence of measured pressure pulsations magnitude upon calculated parameter of stability.

$$\frac{\max grad(t) * \max grad(V)}{dl_{grad}}$$

**Table 3.** Results of calculation and experimental studies

PFR, %	Pulsation magnitude (experimental), A, %	$\frac{\max grad(t) * \max grad(V)}{dl_{grad}} * 10^{-11}$ (calculation)	$\max grad(t)$	$\max grad(V)$	$dl_{grad}$
41	0.019	0.089	238744	5083	0.15
24	0.77	50.09	148592	12463	0.000364
16	0.14	10.7	195250	13474	0.00245
10	0.054	1.02	166370	12548	0.0204
5	0.056	0.0207	198947	5222	0.0501



**Figure 9.** Dependence of pressure pulsations magnitude on. (a) PFR,  $P_{inc} = 330 \text{ kPa}$ ,  $t_{inc} = 340^\circ\text{C}$ ,  $\alpha = 3.0$ . (b) Calculated parameter of stability.

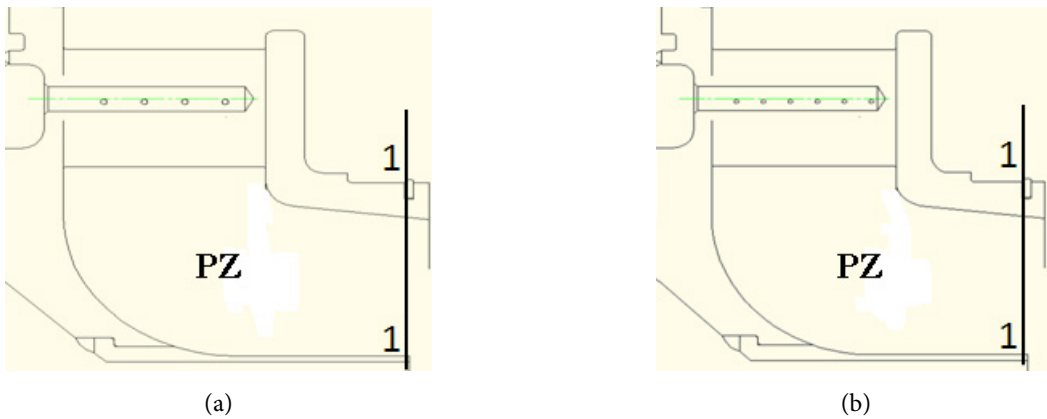


**Figure 10.** Basic versions of BA. (a) With four. (b) With six fuel supply holes into PZ, equispaced along the vane length.

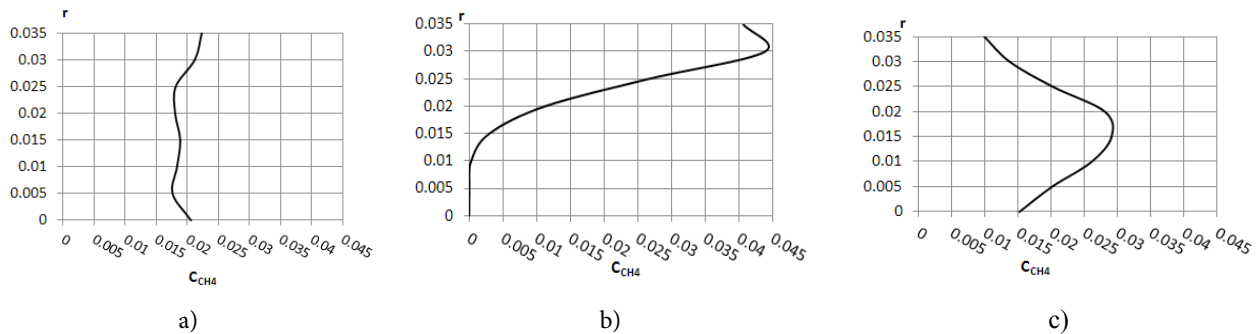


**Figure 11.** Most typical concentration distributions of FAM. (a) Uniform fuel supply. (b) Fuel enrichment to periphery. (c) Fuel enrichment to center.

It is apparent that given values correlate well with each other.

Stability criterion provides an opportunity to perform comparative variants calculations and predict stability of their operation both at different air pressures upstream of C and for various operating condition, reducing time

for experimental development work. Key influence of fuel concentration distribution in outlet section of MB on combustion stability and  $\text{NO}_x$  emission was discovered. Part of fuel supply holes was closed in MB vanes to change concentration distribution. Figure 10 shows two base versions of BA with 4 or 6 fuel supply holes equi-spaced

along the vane length, on basis of which circumferential and radial distortions of FAM were arisen.

Nine versions of fuel distribution in BA were tested in total. Examples of the most typical concentration distributions of FAM are shown in Figure 11.

### 3. Results

Variation of FAM distribution at the outlet of BA changed the zone of stable combustion in case of PB and MB combined operation. For example, Figure 11b shows lines of stable operation in coordinates of excess air ratio and PFR for three options of fuel distribution in BA: uniform fuel supply, enrichment to periphery and enrichment to axis (Figure 11 (a), (b), (c)). It is seen that if C demonstrated stable operation in case of uniform fuel supply at  $25\% \leq \text{PFR} \leq 100\%$  with slight change depending on excess air ratio (the curve is almost horizontal), then in option of enrichment to axis the area of stable operation increased and dependence on excess air ratio is expressed much more stronger: when  $\alpha = 2.7$  stable operation was ensured at  $20\% \leq \text{PFR} \leq 100\%$ , and when  $\alpha = 3.15$  – until termination of fuel flow to PB ( $0\% \leq \text{PFR} \leq 100\%$ ).

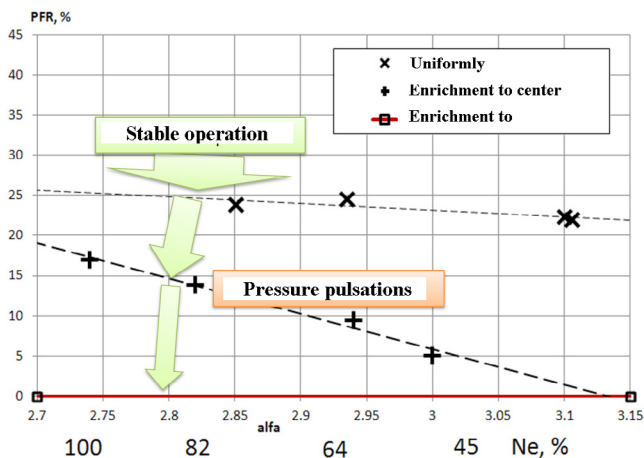


**Figure 12.** Borders of combustor stable operation in case of different options of fuel supply to MB.

In case of fuel enrichment to periphery (Figure 11(b)) during experimental researches operation of C without noise was achieved during combined work of PB and MB with any values of PFR (Figure 12). During these tests effect of concentration profile of FAM on  $\text{NO}_x$  emissions was studied<sup>14</sup>. Calculations and tests enabled to find a technical solution which combined both variants of uniform (Figure 11(a)) and distorted concentration dis-

tribution of FAM (Figure 11(b)), which simultaneously meets the requirements on emissions and stability and does not require significant reworks of equipment. This is the option of radial distribution change of fuel concentration in mode of changeover from PB to MB. For test purpose this option was implemented by installing of collector ring upstream a swirler with precisely directed fuel supply holes as additional fuel channel (AFC) (Figure 13).

As shown by calculations and tests, installation of additional collector has no effect on LEC characteristics both in ignition mode, when only PB works, and in high load mode, when only MB works.

Preliminary algorithm of fuel supply changeover from PB to the Main Fuel Channel (MFC) of MB through AFC is shown in Figure 14. LEC operates only with PB up to 45% Ne, whereat to 60% Ne fuel supply is reduced to 0. Simultaneously with closing of pilot channel, opening of AFC of MB takes place and under 55% load fuel supply starts to MFC of MB. Since 60% Ne fuel supply into AFC is reduced and this increases fuel consumption in MFC. LEC operates up to 100% Ne with variable rate to AFC and MFC of MB. When Ne = 100% fuel is supplied only to MB.  $\text{NO}_x$  emissions and combustion efficiency, measured under such regulation at pressure of 3.5 bar, are shown in Figure 14(b).

### 4. Discussion

LEC tests with an additional fuel channel were carried out at the test bench of the All-Russia Thermal Engineering Institute (JSC “VTI”) at a pressure of 450 kPa and at the test bench of the Baranov Central Institute of Aviation Motor Development (CIAM) at an operating pressure (1500 kPa).

LEC operation only with the pilot burner (PB) was carried out at an excess air ratio of  $\alpha = 10$  and  $\alpha = 3.3$ , which roughly corresponds to the loads ranging from no-load to 50% operation. In this range, the CO emissions do not exceed 300 ppm; completeness of fuel burn-out varies from 99.3% to 99.8%.

Transition to the low-emission mode (from PB to AFC) was performed at  $\alpha = 3.3$  with fuel share in PB ranging from PFR = 100% to PFR = 40%, then at constant PFR = 40% excess air ratio is reduced to  $\alpha = 3.0$  and further transition is carried out at a constant air excess to PFR = 10%. Transition from PFR = 40% to 10% was performed in less than 3 seconds without pressure pulsa-



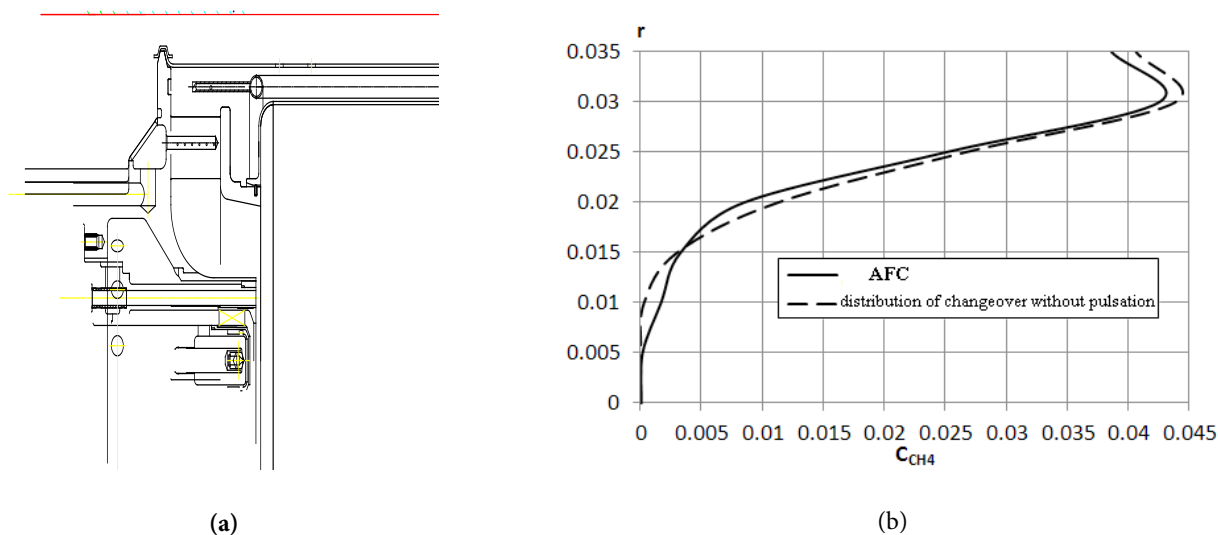


Figure 13. (a) AFC upstream MB. (b) Radial distribution of FAM concentration, obtained using AFC.

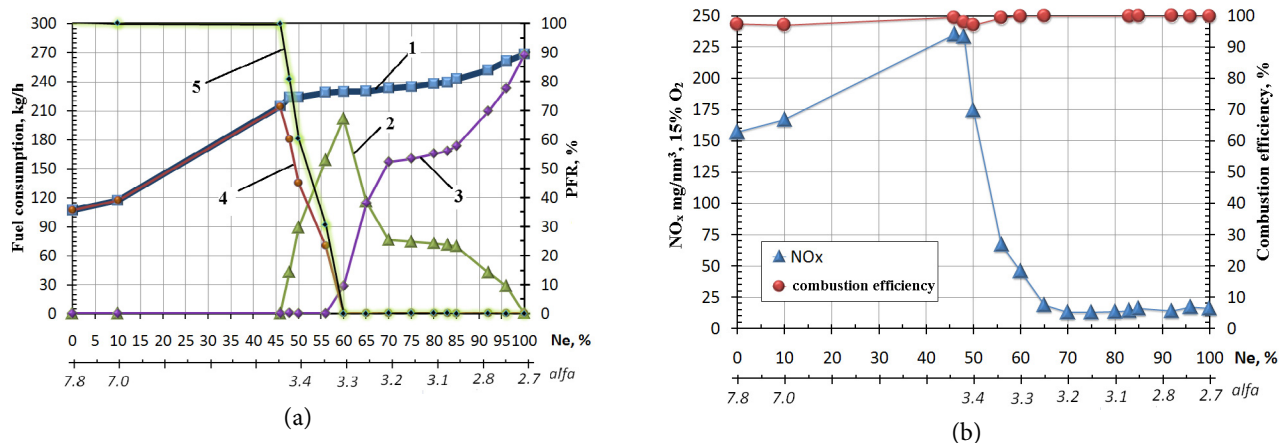


Figure 14. Fuel supply control and LEC emission characteristics. (a) Fuel supply to LEC depending on MFC load: 1- total fuel burn (kg/h), 2- AFC fuel (kg/h), 3- MFC fuel (kg/h), 4- PB fuel (kg/h), 5- PB fuel (%). (b) Dependence of  $NO_x$  emission on MFC load.

tions. Further, the supply of fuel to the pilot burner was terminated completely (PFR = 0).

Fuel distribution between the additional and the main channels of the main burner MFR (AFC and MFC) affects the combustion stability. If MFR values are maintained in a certain range of vibrating combustion does not occur. Low-emission modes are stable, pressure amplitudes do not exceed 0.1% in these modes and the  $NO_x$  concentrations remain within acceptable limits.

Pressure losses in the LEC vary from about ~7.5% at no-load to 5%-5.7% at loads ranging from 50% to 100%.

Lean blowout of the pilot burner occurs at MFR=1, an inlet air temperature  $t_{in} = 380^\circ C$  and  $\alpha = 3.9$ .

When the LEC operates in low-emission mode at  $2.7 < \alpha < 3.3$  temperatures of the flame tube wall do not

exceed  $900^\circ C$ . The highest temperatures are observed near the front FT wall and the mixer holes.

A GTE-110M LEC prototype was manufactured to be installed on the motor. The GTE-110M LEC prototype performance was verified at the JSC "VTI" test bench at 360 kPa air pressure. Transition from PB to AFC was carried out with coefficient at a constant excess air ratio  $\alpha = 3.0 - 3.4$ , inlet air temperature  $t_{in} \sim 380^\circ C$  and inlet air pressure  $P_{IN} \sim 380$  kPa without exceeding the level of pressure pulsations in LEC in the entire transition range. On the basis of the obtained experimental data GTE-110M LEC control algorithm was developed.

Preliminary algorithm of fuel supply changeover from PB to the main fuel channel (MFC) of MB through AFC is shown in Figure 14. LEC operates only with PB up to

45% Ne, whereat to 60% Ne fuel supply is reduced to 0. Simultaneously with closing of pilot channel, opening of AFC of MB takes place and under 55% load fuel supply starts to MFC of MB. Since 60% Ne fuel supply into AFC is reduced and this increases fuel consumption in MFC. LEC operates up to 100% Ne with variable rate to AFC and MFC of MB. When Ne = 100% fuel is supplied only to MB. NO<sub>x</sub> emissions and combustion efficiency, measured under such regulation at pressure of 3.5 bar, are shown in Figure 14(b).

## 5. Conclusion

A low-emission combustion chamber was developed and tested for the GTE-110M gas turbine unit having capacity of 110 MW implementing efficient combustion of 'lean' premixed fuel-air mixture. LEC is designed for installation in the existing motor housing of GTE-110M with minimal modifications.

The GTE-110M LEC was tested at the JSC "VTI" test bench at pressures up to 450 kPa and at the CIAM test bench at an operating pressure (1500 kPa). With the load modes ranging from no-load up to 50% operation CO emissions were <300 mg/m<sup>3</sup>; combustion efficiency exceeded 99.5%. With the load modes ranging from 50% to 100% CO emissions were <10 ppm; combustion efficiency amounted to 99.995%; NO<sub>x</sub> emission was <25 ppv at 15% of O<sub>2</sub>. Pressure losses range from ~7.5% at no-load to 5.7% at loads from 50% to 100%. Relative parameter value for radial outlet gas temperature non-uniformity was  $Q \sim 1.04$ . The wall metal temperature of the flame tube and transition liner does not exceed 800° C. The transition to low-emission mode takes place without vibrating combustion. A GTE-110M LEC control algorithm has been developed.

## 6. Acknowledgments

This study was sponsored by the Ministry of Education and Science of the Russian Federation in line with Agreement No. 14.579.21.0085 dated November 28, 2014; unique identifier for applied scientific research RFMEFI57914X0085.

## 7. References

1. Prade B. Gas turbine operation and combustion performance issues. Janson P. Modern Gas Turbine Systems:

- High efficiency, low emission, fuel flexible power generation. Woodhead Publishing, 2013. P. 383–422. DOI: 10.1533/9780857096067.3.383.
2. Correa SM. A review of NO<sub>x</sub> formation under gas-turbine combustion conditions. *Combustion Science and Technology*. 1992; 87(1):329–62. DOI: 10.1080/00102209208947221.
3. Correa SM. Power generation and aeropropulsion gas turbines: From combustion science to combustion technology. *Proc Combust Inst*. 1998; 27(2):1793–807. DOI: 10.1016/S0082-0784(98)80021-0.
4. Lefebvre AH, Ballal DR. Gas turbine combustion. Alternative fuels and emissions. 3rd ed. CRC Press, Taylor and Francis; 2010.
5. Stöhr M, Boxx I, Carter C, Meier W. Dynamics of lean blowout of a swirl-stabilized flame in a gas turbine model combustor. *Proceedings of the Combustion Institute*. 2011; 33:2953–60. DOI: 10.1016/j.proci.2010.06.103.
6. Billoud G, Galland MA, Huu CH, Candel S. Adaptive active control of combustion instabilities. *Combust Sci and Tech*. 1992; 81:257–83. DOI: 10.1080/00102209208951806.
7. Sattelmayer T. Influence of the combustor aerodynamics on combustion instabilities from equivalence ratio fluctuations. *J Eng Gas Turb Power*. 2002; 125(1):11–9. DOI: 10.1115/1.1365159.
8. Lieuwen T, Yang V, editors. Combustion instabilities in gas turbine engines: operational experience, fundamental mechanisms, and modeling. AIAA. 2006. Available from: <http://dx.doi.org/10.2514/4.866807>
9. Huang Y, Yang V. Dynamics and stability of lean-premixed swirl-stabilized combustion. *Prog Energy Combust Sci*. 2009; 35(4):293–364. Available from: <http://dx.doi.org/10.1016/j.pecs.2009.01.002>
10. Bulysova L, Vasiliev V, Berne A. Methods of experimental data processing of combustion instability. *Energetik*. 2014; 1:55–5.
11. Bulysova L, Vasiliev V, Berne A. Numerical studies of heat emission process in low-emission combustor. *Energetik*. 2012; 9:29–36.
12. Bulysova L, Vasiliev V, Berne A. Numerical studies of pressure effect on the processes of mixing and heat emission in low-emission combustor. *Energetik*. 2013; 3:7–13.
13. Bulysova L, Vasiliev V, Berne A. Effect of flame shape on the combustion stability in a low emission combustor. *Power Technology and Engineering*. 2016; 50(6).
14. Bulysova L, Vasiliev V, Berne A. Effect of air-fuel mixing on NO<sub>x</sub> yield in a low-emission gas turbine plant combustor. *Thermal Engineering*. 2016; 63(4).

## Abbreviations

- CC- Combustion chamber.  
C- combustor.

LEC- Low-emission combustor.

GT- Gas turbine.

FAM- Fuel-air mixture.

BA- Burner arrangement.

FT- Flame tube.

SAH- Secondary air hole.

MB- Main burner.

PB- Pilot burner.

PZ- Premixing zone.

PFR- Part of fuel supplied to pilot burner.

AFC- Additional fuel channel.

MFC- Main fuel channel.

MF- Fuel distribution between the additional and main fuel channels of the Main burner.